Chinese Chemical Letters 34 (2023) 107561

Contents lists available at ScienceDirect

Chinese Chemical Letters

journal homepage: www.elsevier.com/locate/cclet

Discovery and development of tricyclic matrinic derivatives as anti-diabetic candidates by AMPKα activation

Yinghong Li[1], Yuanhui Zhang[1], Tianyu Niu, Yudong Pang, Yulong Shi, Qingxuan Zeng, Jingpu Zhang, Jingyang Zhu, Xiuli Zhong, Yanxiang Wang, Yan Wang, Sheng Tang, Weijia Kong*, Danqing Song*, Jiandong Jiang*

Institute of Medicinal Biotechnology, Chinese Academy of Medical Sciences & Peking Union Medical College, Beijing 100050, China

ARTICLE INFO

Article history:
Received 19 January 2022
Revised 9 May 2022
Accepted 23 May 2022
Available online 27 May 2022

Keywords:
Tricyclic matrinic derivatives
Glucose consumption
Diabetes mellitus
AMP-activated protein kinase (AMPK)

ABSTRACT

We found compound 12*N*-*p*-trifluoromethylbenzenesulfonyl matrinane (**1**) was a potent anti-diabetic agent. Thirty-five tricyclic matrinic derivatives were synthesized and determined for their stimulatory effects on glucose consumption in L6 myotubes, taking **1** as the lead. In high-fat diet (HFD) and STZ induced diabetic mice, **9a** significantly lowers blood glucose, improves glucose tolerance, and especially alleviates diabetic nephropathy and islet damage. Mechanism study indicates that **9a** simultaneously targets mitochondrial complex I to increase AMP/ATP ratio, as well as liver kinase B1 (LKB1) and calcium/calmodulin-dependent protein kinase (CaMKK), which synergistically activates AMPKα and then stimulates glucose transporter 4 (GLUT4) membrane translocation and 2-deoxyglucose (2-DG) uptake to exert anti-diabetic efficacy. Therefore, compound **9a** with a novel structure is a promising anti-diabetic candidate with the advantage of multiple-target mechanism, worthy of further investigation.

Diabetes mellitus (mainly type 2) and related complications are leading causes of morbidity and mortality worldwide. The global market of hypoglycemic drugs expands rapidly, and multiple of hypoglycemic agents such as biguanides, dipeptidyl peptidase-4 (DPP-4) inhibitors, glucagon-likepeptide-1 (GLP-1) receptor agonists, and sodium-glucose co-transporter type 2 (SGLT2) inhibitors are used to treat type 2 diabetes in clinical [1–3]. However, the unignored side effects, such as pancreatitis caused by GLP-1 receptor agonists [4], and acidosis or urinary tract infection induced by SGLT2 inhibitors [5,6] limited their clinical application. Therefore, development of anti-diabetic drugs with high safety profile and novel mechanism is of scientific importance.

Recently, we found that 12*N*-*p*-trifluoromethylbenzenesulfonyl matrinane (**1**, Fig 1), derived from natural product matrine (**2**), displayed promising anti-diabetic effects through suppression of glucose aerobic oxidation and induction of glycolysis with the advantages of high safety profile and ameliorating diabetic nephropathy [7]. In order to develop a new type of hypoglycemic candidates, a series of tricyclic matrinic analogues was continuously synthesized to expand the glucose-lowering structure-activity relationship and in-depth mechanism research of its kind.

According to the primary structure-activity relationship (SAR) analysis, 11-butane side chain was beneficial for activity [7]. SAR investigation was mainly focused on the substitution on the 12*N* atom in this study while 11-side chain was set as lipophilic butane or bulky ester and amide moiety, by which a panel of tricyclic matrinic analogues (Table 1) were prepared. All the target compounds were tested *in vitro* for their ability to stimulate glucose consumption in skeletal muscle L6 cell, and the druglike property, *in vivo* hypoglycemic effect as well as mode of action of the key compound were illustrated in this study.

A total of 35 tricyclic matrinic analogues, of which 26 were new, were prepared from **2**, as depicted in Scheme 1. Compounds **9a–e**, **12a**, **12b**, **12d** and **14a** were prepared as we described [8–12]. The key intermediate matrinane **8** was acquired from **2** through a seven-step procedure in a good yield as reported previously [8], and the aimed 12*N*-substituted matrinane derivatives **9f–x** were obtained from an electrophilic substitution reaction of **8** in 33%–73% yields [8–10,13]. Target compounds **12a–g** and **14a–d** were gained from a two-step sequence reaction from intermediates **10a–d**, respectively [11,12].

All target compounds were evaluated for their stimulatory efficacy on glucose consumption at the concentration of 20 μmol/L in

* Corresponding authors.
E-mail addresses: kongweijia@imb.pumc.edu.cn (W. Kong), songdanqing@imb.pumc.edu.cn (D. Song), jiang.jdong@163.com (J. Jiang).
[1] These authors contributed equally to this work.

https://doi.org/10.1016/j.cclet.2022.05.075
1001-8417/

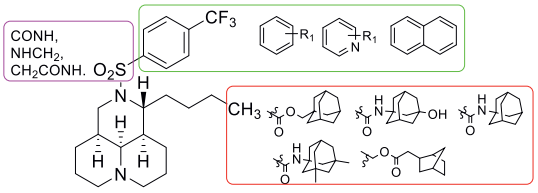

1 G_X/G_{DMSO}: 1.49 (25 μmol/L in Hep G2)

Fig. 1. Chemical structure and modification of lead **1**.

L6 rat skeletal muscle cells, taking **1** (20 μmol/L) and metformin (MET, 5 mmol/L) as the positive controls. The activity was identified as the ratio of G_x /G_{DMSO}. The structures and activities of all target compounds were listed in Table 1.

Our previous SAR study disclosed that the *p*-CF_3 on the benzene ring (**1**) owned higher activity than *o*-CF_3 [8], then compound **9a** with *m*-CF_3 was generated and gave a superior activity to the lead **1** and MET (5 mmol/L), with the G_x/G_{DMSO} value of 1.35. However, compounds **9b–e** with various of other substitutions on the benzene ring gave significantly declined activities, indicating CF_3 might be beneficial for the activity.

Table 1
The structures and glucose consumptions of target compounds in L6 myotubes.

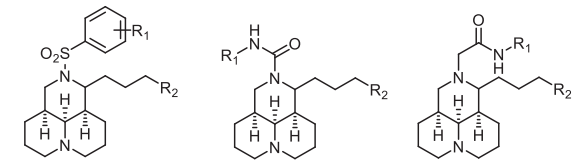

No	R_1	R_2	Gx/G_{DMSO}	No	R_1	R_2	Gx/G_{DMSO}
1	*p*-CF_3	CH_3	1.25 ± 0.01	**9s**	4-Br-2-ClC_6H_3	CH_3	0.73 ± 0.04
9a*	*m*-CF_3	CH_3	1.35 ± 0.01	**9t**	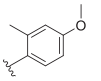	CH_3	0.70 ± 0.03
9b*	*m*-CN	CH_3	1.05 ± 0.013	**9u**		CH_3	0.72 ± 0.08
9c*	2,2,4-tri-OCH_3	CH_3	1.02 ± 0.03	**9v**	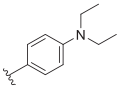	CH_3	0.65 ± 0.06
9d*	*p*-$NHCOCH_3$	CH_3	1.08 ± 0.04	**9w**	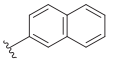	CH_3	0.64 ± 0.05
9e*	*p*-$COCH_3$	CH_3	1.02 ± 0.02	**9x**		CH_3	0.67 ± 0.01
9f	C_6H_5	CH_3	1.18 ± 0.05	**12a***	*m*-CF_3	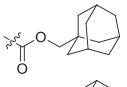	1.22 ± 0.12
9g	*p*-EtC_6H_4	CH_3	1.27 ± 0.05	**12b***	*p*-CH_3	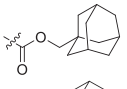	1.16 ± 0.01
9h	*m*-$OCH_3C_6H_4$	CH_3	1.02 ± 0.02	**12c**	*p*-OCH_3	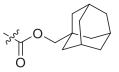	1.20 ± 0.04
9i	*m*-ClC_6H_4	CH_3	1.08 ± 0.02	**12d***	H	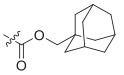	1.13 ± 0.04
9j	*p*-ClC_6H_4	CH_3	1.22 ± 0.01	**12e**	*m*-CF_3	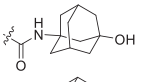	1.08 ± 0.02
9k	2,4-di-FC_6H_3	CH_3	1.12 ± 0.02	**12f**	*m*-CF_3	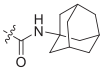	1.07 ± 0.01
9l	3,5-di-ClC_6H_3	CH_3	1.02 ± 0.03	**12g**	*p*-CF_3	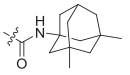	1.06 ± 0.01
9m	Cyclohexyl	CH_3	1.16 ± 0.03	**14a***	*m*-CF_3	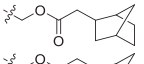	0.82 ± 0.01
9n	Cyclopentyl	CH_3	0.63 ± 0.07	**14b**	*p*-CH_3	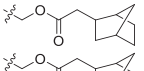	1.11 ± 0.04
9o	*p*-$OCH_3C_6H_4CH_2$	CH_3	1.12 ± 0.04	**14c**	*p*-OCH_3	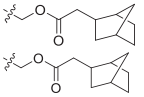	1.07 ± 0.03
9p	2-Cl-4-FC_6H_3	CH_3	0.63 ± 0.07	**14d**	H	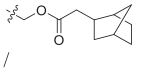	1.07 ± 0.02
9q	5-Br-2-FC_6H_3	CH_3	0.90 ± 0.13	**MET**	/	/	1.30 ± 0.13
9r	4-FC_6H_4	CH_3	0.69 ± 0.07				

*: Known compounds.

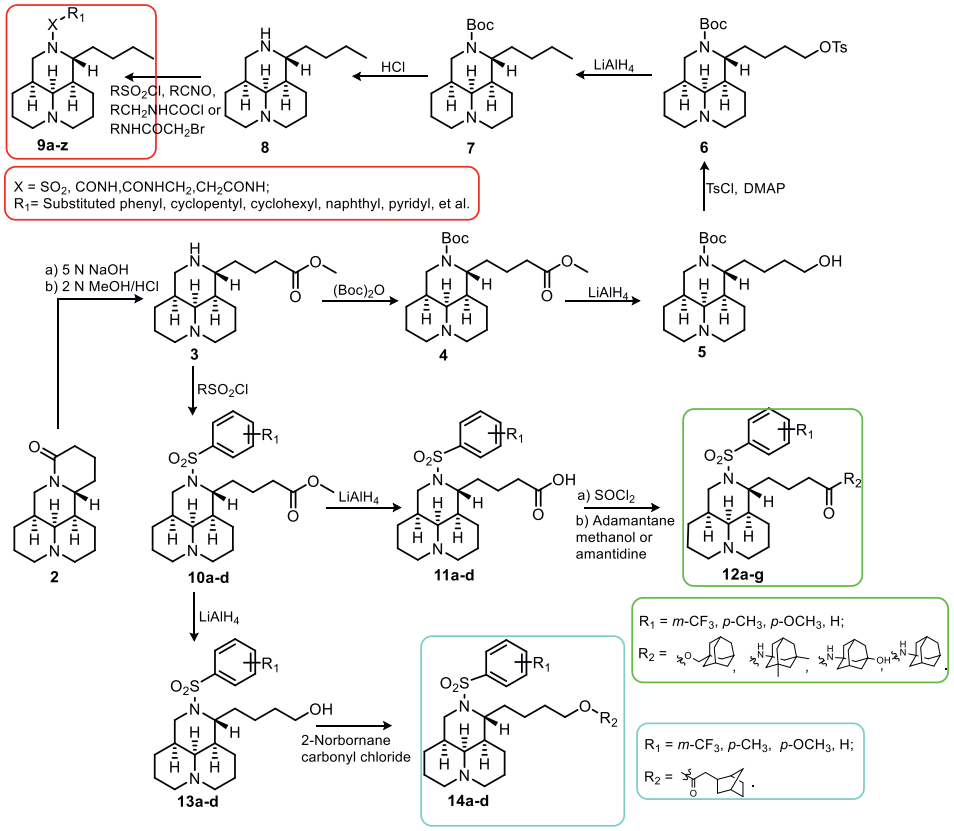

Scheme 1. The synthesis of all target compounds.

Then, the sulfonyl linker was replaced by aminocarbonyl linker, and compounds **9f–o** with a benzene ring were synthesized and evaluated. Except for compounds *p*-Et (**9g**) and *p*-chloro (**9j**) gave a comparable activity to **1**, all other compounds gave decreased activities to varying degrees. The alternation of benzene ring into cyclohexyl (**9m**) or cyclopentyl (**9n**) ring led to comparable or declined activities. The alternation of aminocarbonyl into metheneaminocarbonyl or aminocarbonylmethene also brought descended activities, as seen in **9o** or **9p–x**.

In addition, compounds **12a–g** with a lipophilic bulky 11-side chain were obtained. Compounds **12a–d** with an adamantly ester moiety gave comparable or slightly inferior activities to the lead **1**. The alternation of ester bond into amide bond gave decreased activities, as seen in compounds **12e–g**. Meanwhile, another series of matrinyl 2-norbornane acetates **14a–c** displayed inferior activities too, indicating the replacement of 11-butane into the bulky ester or amide moiety was unfavorable for activity.

Then the glucose consumption-stimulating activities of **9a** at different concentrations (10, 20 and 40 μmol/L) were verified in L6 myotubes, HepG2 cells and 3T3-L1 cells, taking **1** as the positive control. It dose-dependently promoted glucose consumption in all three cells (Fig. S1 in Supporting information), and the efficacies were higher than those of **1** when administered at a same concentration.

Then the druglike property of **9a** was evaluated. In acute toxicity test, it gave the median lethal dose (LD_{50}) values of over 1000 mg/kg *via* oral route, comparable to that of lead **1** [8], as well as the LD_{50} values of 400 mg/kg and over 40 mg/kg *via* intraperitoneal and intravenous routes respectively. And it gave the LD_{50} value between 50–60 μmol/L in the zebrafish embryonic developmental toxicity assay (Fig. S2 in Supporting information). The PK profiles of compound **9a** was investigated in SD rat model at the dosage of 25 mg/kg *via* oral route. As depicted in Table S1 and Fig. S3 (Supporting information), it gave the $T_{1/2}$ value of 4.03 h, maximum concentration (C_{max}) of 1.04 μmol/L, area under curve (AUC) of 7.36 μmol h/L, and an oral bioavailability of 16.7%. These results suggested that **9a** owned a high druglike profile**.**

The beneficial effects of **9a** on glucose metabolism were evaluated in a high-fat diet (HFD) + STZ-induced diabetic mouse model. The research committee of the Institute of Medicinal Biotechnology reviewed and approved the protocols of the animal experiments. Animals were treated humanely and cared for according to the guidelines of CAMS&PUMC. As shown in Table S2 (Supporting information), the diabetic model was developed successfully before treatment. After 8 weeks of administration, the fasting blood glucose (FBG) values of the diabetic mice were lowered by **9a** dose-dependently. It lowered FBG at 100 mg/kg to an extent similar to that of MET at 300 mg/kg, comparable to **1**'s efficacy in KK-Ay mice [8]. The decreased serum insulin level was greatly restored by **9a**, and **9a** at 50 mg/kg gave a comparable efficacy to **1** at 100 mg/kg in KK-Ay mice [8]. It also restored the liver and kidney functions by reducing serum creatinine (Scr), alanine aminotransaminase (ALT), aspartate aminotransferase (AST) and total bile acid (TBA) levels, similar to those of MET.

In oral glucose tolerance test (OGTT), the HFD + STZ induced diabetic mice had impaired glucose tolerance as compared to normal control. Compound **9a** improved glucose tolerance of the diabetic mice significantly and dose-dependently (Figs. 2A and B), the activities of **9a** at 50 mg/kg were comparable to those of **1** at 100 mg/kg in KK-Ay mice [8], and the activities of **9a** at 100 mg/kg were comparable to those of MET at 300 mg/kg. Significant abnormalities appeared in the kidney of diabetic mice (Fig. 2C), which included glomerular sclerosis and tubulointerstitial lesions (Figs. 2D and E), and these pathological changes were greatly ameliorated by **9a** administration (Figs. 2C– E), in a comparable efficacy to **1** in KK-Ay mice [8].

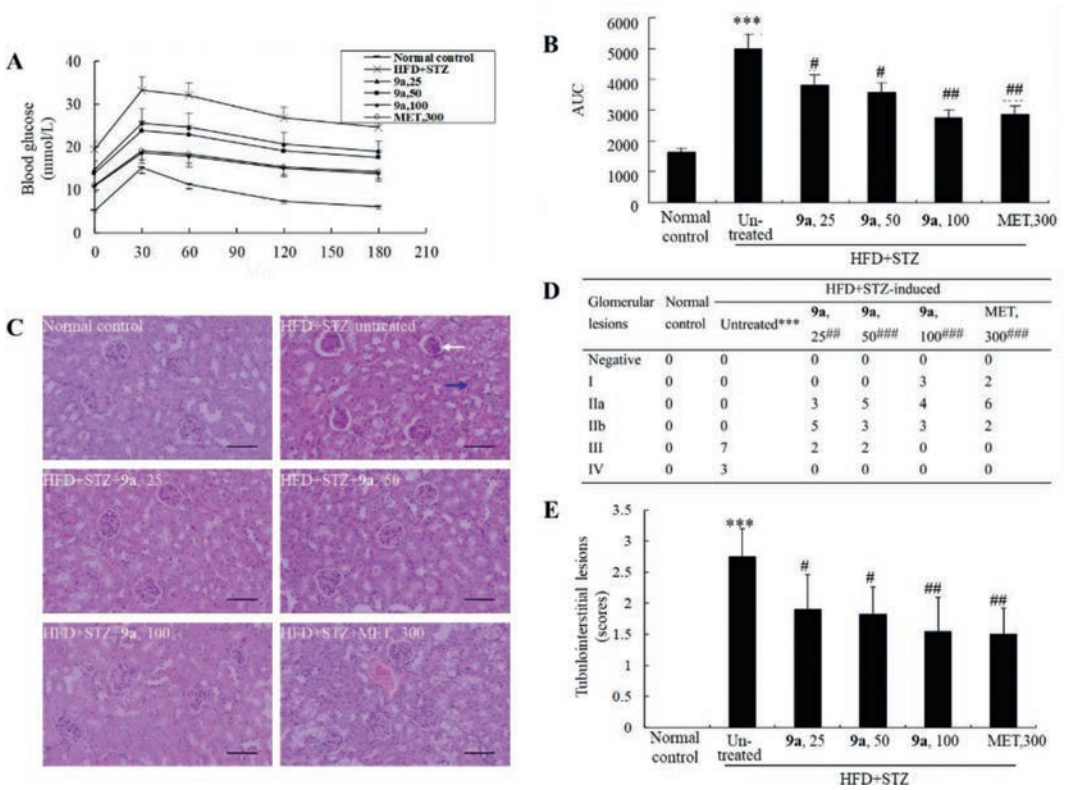

Fig. 2. (A, B) Effects of **9a** on OGTT in HFD + STZ-induced diabetic mice. (C-E) Effects of **9a** on pathological changes of kidney in HFD + STZ-induced diabetic mice (200×, scale bar = 100 μm). The white arrow indicates glomerular lesions and the blue arrow indicates tubulointerstitial lesions. Values are mean ± SD of 10 mice of each group in panel C. $^{***}P < 0.001$ *vs.* that of normal control group; $^{\#}P < 0.05$, $^{\#\#}P < 0.01$, $^{\#\#\#}P < 0.01$ *vs.* that of untreated diabetic mice.

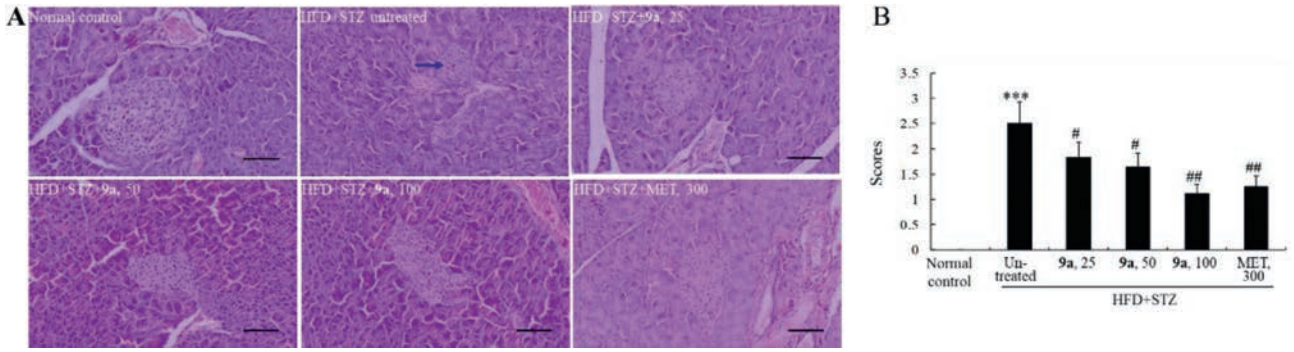

Fig. 3. Effects of **9a** on pathological changes of pancreas in HFD + STZ-induced diabetic mice (200×, scale bar = 100 μm). Typical images are presented panel A, in which a blue arrow indicates the atrophy of islet. The scores of pathological changes are presented in panel B, in which values are mean ± SD of 10 mice in each group. $^{***}P < 0.001$ *vs.* normal control group; $^{\#}P < 0.05$, $^{\#\#}P < 0.01$ *vs.* untreated diabetic mice.

Meanwhile, the islets of the diabetic mice largely atrophied accompanied with structure disorder due to STZ injection (Fig. 3). Compound **9a** significantly improved the abnormalities of islets, in a comparable efficacy to **1** in KK-Ay mice (Fig. 3) [8]. As the positive control, the efficacies of MET at 300 mg/kg were similar to those of **9a** at 100 mg/kg.

Next, the detailed anti-diabetic mechanism of **9a** was explored. First, the influence of **9a** on glucose uptake was evaluated in L6 myotubes. As shown in Fig. 4A, at concentrations of 10, 20, and 40 μmol/L, **9a** greatly stimulated the uptake of 2-DG, a glucose analogue, to about 6.73 to 8.64-fold of DMSO-treated cells. Then, cellular localization of glucose transporter 4 (GLUT4) was assayed by immunofluorescence staining. As shown in Fig. 4B, GLUT4 protein (green) was mainly localized in cytoplasm in DMSO-treated cells. After **9a** treatment, the surface level of GLUT4 increased in a concentration-dependent manner, indicating that it promoted GLUT4 membrane translocation in L6 myotubes, similar to those of MET. These results indicate that **9a** increases glucose uptake and GLUT4 membrane translocation in L6 myotubes.

In light of the crucial role of AMP-activated protein kinase (AMPK) in GLUT4 membrane translocation [14,15], the stimulatory effect of **9a** upon AMPK was investigated in L6 myotubes, taking MET as the positive control. As shown in Fig. S4A (Supporting information), compound **9a** stimulated AMPKα phosphorylation in a dose-dependent manner, as indicated by the significant increase of *p*-AMPKα (Thr172) level after treatment, and the stimulatory efficacy of **9a** at 40 μmol/L was comparable to that of MET at 5 mmol/L. In addition, the stimulatory effects of **9a** on AMPKα phosphorylation were completely blocked by compound **C**, a selective AMPK inhibitor, as shown in Fig. S4B (Supporting information). Accordingly, the promoting activities of **9a** on GLUT4 membrane translocation (Fig. 5A) and 2-DG uptake (Fig. 5B) were also abol-

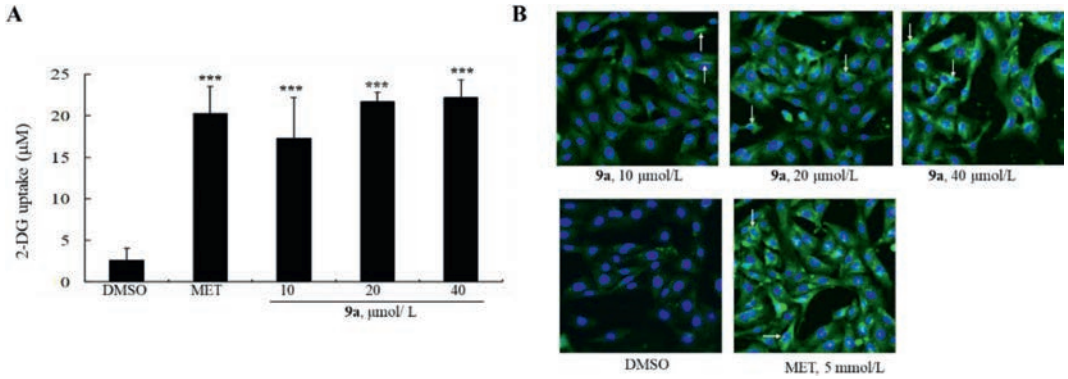

Fig. 4. Effects of **9a** on 2-DG uptake (A) and GLUT4 translocation (B). Values are ± SD of 4 repeated experiments, $^{***}P < 0.001$ *vs.* DMSO-treated cells. GLUT4 membrane translocation was determined by immunofluorescence assay (green) and DAPI was used to stain nucleus (blue). The white arrows indicate membrane localization of GLUT4 protein. One of 3 repeated experiments (×100) is presented in panel B.

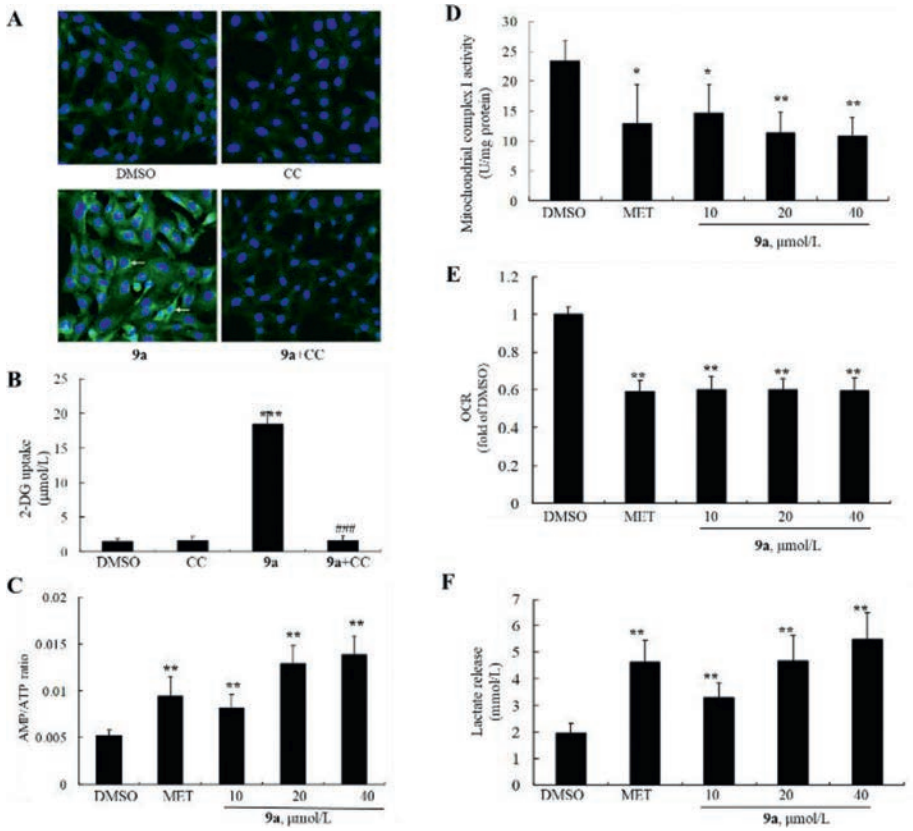

Fig. 5. (A, B) Blocking effects of CC on GLUT4 translocation (×100) and 2-DG uptake. Values are mean ± SD of 4 repeated experiments, $^{***}P < 0.001$ *vs.* DMSO-treated cells, $^{\#\#\#}P < 0.001$ *vs.* cells treated with **9a** alone. (C) Effects of **9a** on AMP/ATP ratio. (D) Effects of **9a** on mitochondria complex I activity. (E) Effects of **9a** on OCR. (F) Effects of **9a** on lactate release. For C-F, values are mean ± SD 3-4 repeated experiments. $^{*}P < 0.05$, $^{**}P < 0.01$ *vs.* DMSO-treated cells.

ished in the presence of compound **C** in L6 myotubes, similar to that of MET. These results suggest that AMPKα is indispensable for the stimulatory effects of **9a** on glucose metabolism.

AMPK could be activated by the increase of AMP/ATP ratio or upstream AMPK kinases (AMPKKs) [16,17]. First, the influence of **9a** on AMP/ATP ratio was evaluated in L6 myotubes. It increased AMP/ATP ratio in a dose-dependent manner, as disclosed in Fig. 5C. Mitochondrial complex I plays a crucial role in ATP production [18,19], as anticipated, **9a** suppressed mitochondrial complex I activity dose-dependently (Fig. 5D). Accordingly, as shown in Figs. 5E and F, it also decreased cell oxygen consumption rate (OCR), and promoted cellular lactate release, in agreement of **1**'s effects in our earlier study [8].

Next, its influences on upstream AMPKKs, namely liver kinase B1 (LKB1) and calcium/calmodulin-dependent protein kinase (CaMKK) [17], were investigated. It greatly increased the phosphorylation level of LKB1 at Ser334 (Fig. S4A). In HeLa cells with LKB1-deficency [20], its stimulation on AMPKα phosphorylation were abolished (Fig. 6A). STO-609 (a CaMKK inhibitor) was used to evaluate the role of CaMKK in the AMPK-stimulating activity of **9a**. As shown in Fig. 6B, the stimulating activities of **9a**, MET, as well as ionomycin, an ionophore for calcium, on AMPKα phosphorylation were totally blocked in the presence of STO-609. Therefore, **9a** activates AMPKα in a AMPKKs-dependent manner.

In summary, 35 tricyclic matrinic derivatives, of which 26 are new, are synthesized and determined for their stimulation effects

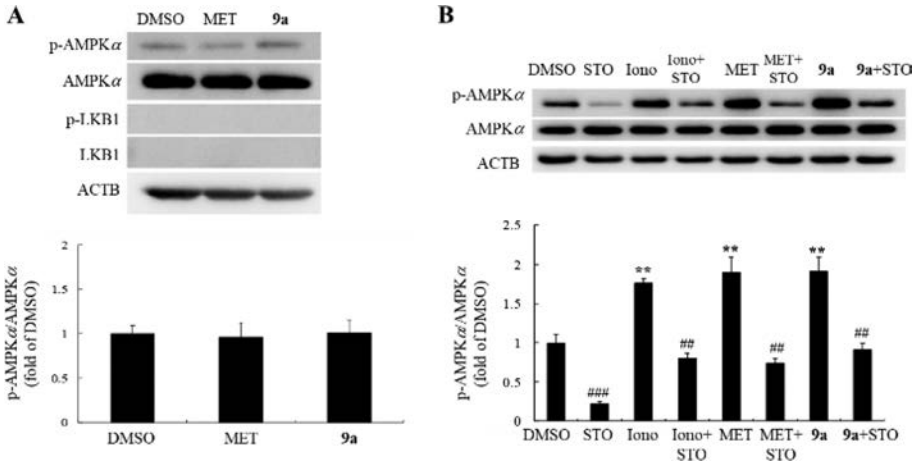

Fig. 6. (A) Effects of **9a** on the phosphorylation of AMPKα in HeLa cells. (B) Blocking effect of STO-609 (STO) on AMPKα phosphorylation. Values are mean ± SD of 3 repeated experiments. $^{**}P < 0.01$ *vs.* DMSO-treated cells, $^{\#\#}P < 0.01$, $^{\#\#\#}P < 0.001$ *vs.* same-treated cells without STO.

on glucose consumption in L6 myotubes, taking **1** as the lead. The most potent compound **9a**, with a highly druglike feature, effectively lowers blood glucose and ameliorates diabetic nephropathy and islet damage in HFD and STZ induced diabetic mice. Compared to **1**, it exerts comparable potencies on restoring serum insulin level and improving glucose tolerance at a lower dosage. The mechanism study indicates that compound **9a** increases AMP/ATP ratio through inhibiting mitochondrial complex I and affects LKB1 and CaMKK, which synergically induces AMPKα activation and successively stimulates GLUT4 membrane translocation and 2-DG uptake to accelerate glucose consumption. Our results suggest that compound **9a** may be a potential novel anti-diabetic candidate with the advantage of multiple-target mechanism, worthy of further investigation.

Declaration of competing interest

The authors declare that they have no known competing financial interests or personal relationships that could have appeared to influence the work reported in this paper.

Acknowledgments

This work was supported by CAMS Innovation Fund for Medical Sciences (No. 2021-12M-1-030), the Natural Science Foundation of Beijing Municipality (No. 7202131) and Chinese Pharmaceutical Association-Yiling Pharmaceutical Innovation Fund for Biomedicine (No. GL-1-B04-20190397).

Supplementary materials

Supplementary material associated with this article can be found, in the online version, at doi:10.1016/j.cclet.2022.05.075.

References

[1] E.M. Vaughan, J.J. Rueda, S.L. Samson, et al., Curr. Diabetes Rev. 16 (2020) 851–858.
[2] Z.G. Sun, Z.N. Li, H.L. Zhu, Mini Rev. Med. Chem. 20 (2020) 1709–1718.
[3] S. Cornell, J. Clin. Pharm. Ther. 45 (Suppl. 1) (2020) 17–27.
[4] E. Brown, H.J.L. Heerspink, D.J. Cuthbertson, et al., Lancet 398 (2021) 262–276.
[5] G. Savarese, B. Schrage, F. Cosentino, et al., ESC Heart Fail. 7 (2020) 3438–3451.
[6] M. Singh, A. Kumar, Curr. Drug Saf. 13 (2018) 84–91.
[7] S. Tang, C. Wang, Y.H. Li, et al., Eur. J. Med. Chem. 201 (2020) 112315.
[8] S. Tang, Y.H. Li, X.Y. Cheng, et al., Future Med. Chem. 8 (2016) 495–508.
[9] X.Y. Cheng, Y.H. Li, S. Tang, et al., Eur. J. Med. Chem. 126 (2017) 133–142.
[10] S.G. Wang, L.Y. Kong, Y.H. Li, et al., Bioorg. Med. Chem. Lett. 25 (2015) 3690–3693.
[11] T. Niu, X. Zhao, J. Jiang, et al., Molecules 24 (2019) 921.
[12] J. Jiang, X. Zhao, T. Niu, et al., Pharmazie 74 (2019) 265–269.
[13] S. Tang, Z.G. Peng, X. Zhang, et al., Chin. Chem. Lett. 27 (2016) 1052–1057.
[14] F. Dehghan, F. Hajiaghaalipour, A. Yusof, et al., Sci. Rep. 6 (2016) 25139.
[15] J.O. Lee, S.K. Lee, J.H. Kim, et al., J. Biol. Chem. 287 (2012) 44121–44129.
[16] S. Herzig, R.J. Shaw, Cell Biol. 19 (2018) 121–135.
[17] A. Gormand, E. Henriksson, K. Ström, et al., J. Cell Biochem. 112 (2011) 1364–1375.
[18] K. Fiedorczuk, L.A. Sazanov, Trends Cell Biol. 28 (2018) 835–867.
[19] H. Zhu, B. Zhang, N. Zhu, et al., Chin. Chem. Lett. 32 (2021) 1220–1223.
[20] J. Han, J. Yi, F. Liang, et al., Mol. Cell Endocrinol. 405 (2015) 63–73.